JOURNAL OF VIROLOGY, Dec. 2004, p. 13019–13027 Vol. 78, No. 23
0022-538X/04/$08.00+0 DOI: 10.1128/JVI.78.23.13019–13027.2004

Structural Protein Requirements in Equine Arteritis Virus Assembly

Roeland Wieringa,[1]† Antoine A. F. de Vries,[2] Jannes van der Meulen,[3] Gert-Jan Godeke,[1]‡ Jos J. M. Onderwater,[3] Hans van Tol,[4] Henk K. Koerten,[3] A. Mieke Mommaas,[3] Eric J. Snijder,[4] and Peter J. M. Rottier[1]*

Virology Division, Department of Infectious Diseases and Immunology, Faculty of Veterinary Medicine, and Institute of Biomembranes, Utrecht University, Utrecht,[1] and Gene Therapy Section[2] and Center for Electron Microscopy,[3] Department of Molecular Cell Biology, and Molecular Virology Laboratory, Department of Medical Microbiology, Leiden University Medical Center, Leiden,[4] The Netherlands

Received 4 May 2004/Accepted 20 July 2004

Equine arteritis virus (EAV) is an enveloped, positive-stranded RNA virus belonging to the family *Arteriviridae* of the order *Nidovirales*. EAV particles contain seven structural proteins: the nucleocapsid protein N, the unglycosylated envelope proteins M and E, and the N-glycosylated membrane proteins GP_{2b} (previously named G_S), GP_3, GP_4, and GP_5 (previously named G_L). Proteins N, M, and GP_5 are major virion components, E occurs in virus particles in intermediate amounts, and GP_4, GP_3, and GP_{2b} are minor structural proteins. The M and GP_5 proteins occur in virus particles as disulfide-linked heterodimers while the GP_4, GP_3, and GP_{2b} proteins are incorporated into virions as a heterotrimeric complex. Here, we studied the effect on virus assembly of inactivating the structural protein genes one by one in the context of a (full-length) EAV cDNA clone. It appeared that the three major structural proteins are essential for particle formation, while the other four virion proteins are dispensable. When one of the GP_{2b}, GP_3, or GP_4 proteins was missing, the incorporation of the remaining two minor envelope glycoproteins was completely blocked while that of the E protein was greatly reduced. The absence of E entirely prevented the incorporation of the GP_{2b}, GP_3, and GP_4 proteins into viral particles. EAV particles lacking GP_{2b}, GP_3, GP_4, and E did not markedly differ from wild-type virions in buoyant density, major structural protein composition, electron microscopic appearance, and genomic RNA content. On the basis of these results, we propose a model for the EAV particle in which the $GP_{2b}/GP_3/GP_4$ heterotrimers are positioned, in association with a defined number of E molecules, above the vertices of the putatively icosahedral nucleocapsid.

Equine arteritis virus (EAV) is the prototypic member of the *Arteriviridae* family (order *Nidovirales*), which also includes lactate dehydrogenase-elevating virus (LDV), porcine reproductive and respiratory syndrome virus (PRRSV), and simian hemorrhagic fever virus (4). Virus particles have a diameter of approximately 60 nm and consist of a 12.7-kb RNA genome of positive polarity that is packaged by the 14-kDa nucleocapsid protein (N) into a putatively icosahedral core, which is surrounded by a lipid-containing envelope with small surface projections (17, 20).

In the EAV envelope six viral proteins have been identified (6, 27, 43). The 16-kDa unglycosylated membrane protein M and the heterogeneously glycosylated GP_5 (previously named G_L) protein of 30 to 42 kDa are the most abundant envelope proteins and occur in virions as covalently linked heterodimers (7, 26). The membrane topology of the EAV M protein is unknown but its hydropathy profile resembles that of the LDV M protein. The latter protein was previously shown to be a triple-spanning membrane protein having its amino terminus at the outside of the virion and its carboxy terminus at the inside (12). The EAV M protein is, therefore, assumed to contain three internal transmembrane segments as well, leaving a short 19-amino-acid N-terminal domain exposed at the surface of the virion and an approximately 72-residue C-terminal domain buried within the virus interior (6, 25). Also, the membrane topology of the EAV GP_5 protein has not been elucidated yet. Again, by analogy to the situation in LDV (12), the glycosylated N-terminal half of the EAV GP_5 protein is thought to comprise the approximately 95-residue ectodomain, while the C-terminal half consists of three membrane-spanning domains followed by an endodomain of about 64 amino acids (6).

The GP_{2b} (previously named G_S), GP_3, and GP_4 proteins are all minor envelope glycoproteins (6, 43). Recently, we demonstrated that these proteins occur in virions as a covalently associated heterotrimeric complex (42). Both the GP_{2b} and the GP_4 protein are type I membrane proteins with relatively small endodomains. They contain one and three functional N-glycosylation sites, respectively (8, 43). The membrane topology of GP_3 is less obvious. As its hydrophobic amino terminus is not cleaved, the protein may be inserted into the viral membrane by either or both of its hydrophobic terminal domains (16, 43). Furthermore, the GP_3 protein has no appreciable endodomain and contains six putative N-glycosylation sites, most or all of which are used (16, 43). The small hydrophobic envelope protein (E) of 6.5 to 10.5 kDa does not contain N-linked glycans and has been detected in virus parti-

* Corresponding author. Mailing address: Virology Division, Department of Infectious Diseases and Immunology, Yalelaan 1, 3584 CL Utrecht, The Netherlands. Phone: 31 30 2532463. Fax: 31 30 2536723. E-mail: p.rottier@vet.uu.nl.

† Present address: Gene Therapy Section, Department of Molecular Cell Biology, Leiden University Medical Center, Leiden, The Netherlands.

‡ Present address: Microbiological Laboratory for Health Protection, National Institute for Public Health and the Environment, Bilthoven, The Netherlands.

cles in higher amounts than the minor envelope glycoproteins but in lower quantities than the GP_5 and M proteins (27). The E, GP_{2b}, GP_3, GP_4, GP_5, M, and N proteins are encoded by open reading frames (ORFs) 2a, 2b, 3, 4, 5, 6, and 7, respectively. By separately knocking out the expression of each of these ORFs in the context of a (full-length) EAV cDNA clone, it has been shown that all seven structural proteins are required for the production of infectious progeny virus (21, 27, 32).

The assembly of EAV takes place at membranes of the endoplasmic reticulum (ER), the intermediate compartments, and/or the Golgi complex (20), but little is known about the molecular interactions involved in EAV budding. The available infectious EAV cDNA clones (15, 32) provide valuable systems for studying the roles of the viral structural proteins in EAV assembly, particularly because they allow analysis of not only viable but, importantly, also nonviable virus mutants. Accordingly, in this report, gel electrophoresis, immunoprecipitation, and ultracentrifugation analyses and electron microscopy were used to study the effects on virus assembly of inactivating each of the structural protein genes separately in the context of a (full-length) EAV cDNA clone. These experiments revealed that N, M, and GP_5 are the only structural proteins required for the production of viral particles. Furthermore, no differences in the major structural protein composition, buoyant density, and morphology were observed between wild-type (WT) virions and the viral particles generated in the absence of E, GP_{2b}, GP_3, or GP_4.

MATERIALS AND METHODS

Cells, antibodies, and plasmids. Baby hamster kidney cells (BHK-21 C13) cells (American Type Culture Collection) were grown and maintained in Glasgow minimal essential medium (GMEM; Invitrogen-Life Technologies), supplemented with 10% heat-inactivated fetal bovine serum (FBS), 100 IU of penicillin per ml, and 100 μg of streptomycin per ml (GMEM–10% FBS). The production and characterization of polyclonal antisera directed against the EAV E, GP_{2b}, GP_3, GP_4, M, and N proteins (designated αE, αGP_{2b}, αGP_3, αGP_4, αM, and αN, respectively) have been reported previously (6, 27, 38, 43). The monoclonal antibodies (MAbs) 93B, 51A, and E1A19, which are specific for GP_5 (93B) and N (51A and E1A19) have been described elsewhere (14, 38). The generation of the different EAV cDNA clones has also been reported earlier (21, 27, 32).

RNA transcription and transfection and metabolic labeling of intracellular proteins. The in vitro synthesis and transfection of genome-length EAV RNAs and the metabolic labeling of intracellular proteins have been performed essentially as described previously (41).

Preparation of radiolabeled viral particles. BHK-21 C13 cells were transfected with synthetic EAV RNAs and labeled at 7 h posttransfection (p.t.) with L-[^{35}S]methionine or L-[^{35}S]cysteine by using a standard procedure (41). After a 12-h labeling period at 39°C, the culture supernatant was harvested, and the cell debris was removed by low-speed centrifugation (10 min at 1,700 × *g* and room temperature [RT] in a microcentrifuge). The viral particles were then pelleted through a cushion of 20% (wt/wt) sucrose in TM (20 mM Tris-HCl [pH 7.6]–20 mM $MgCl_2$) by centrifugation for 2 h in an SW 50.1 rotor (Beckman) at 28,000 rpm and 4°C. The resulting pellet was dissolved in 1 ml of ice-cold lysis buffer (20 mM Tris-HCl [pH 7.6], 150 mM NaCl, 1% NP-40, 0.5% sodium deoxylcholate, 0.1% sodium dodecyl sulfate [SDS], 20 mM *N*-ethylmaleimide [Sigma-Aldrich], and 1 μg each of aprotinin, leupeptin, and pepstatin A per ml) and further processed as a true cell lysate. Alternatively, the culture supernatants were centrifuged for 10 min at 1,700 × *g* and RT in a microcentrifuge to remove cell debris. The resulting supernatants were mixed with a one-fourth volume of 5× lysis buffer (100 mM Tris-HCl [pH 7.6], 150 mM NaCl, 5% NP-40, 2.5% sodium deoxylcholate, 0.5% SDS, 100 mM *N*-ethylmaleimide containing 5 μg each of aprotinin, leupeptin, and pepstatin A per ml), and the samples were further processed as described for the cell lysates (42).

Sucrose density gradients. For sucrose density gradient analysis, cleared culture supernatants (400 μl) of BHK-21 C13 cells transfected with synthetic EAV RNAs were loaded onto 20 to 50% (wt/wt) sucrose gradients made up in 20 mM Tris-HCl (pH 7.6)–100 mM NaCl–1 mM EDTA. The gradients were subjected to centrifugation for 16 h at 30,000 rpm and 4°C by using an SW 41 rotor (Beckman) and collected in 15 serial fractions of 750 μl from the bottom of the centrifugation tubes. Next, a one-fourth volume of 5× lysis buffer was added to each fraction. The samples were cleared by centrifugation for 15 min at 20,880 × *g* and 4°C in a microcentrifuge. The pellets were discarded, and the supernatants were supplemented with EDTA to a final concentration of 5 mM.

Immunoprecipitation and gel electrophoresis. Proteins were immunoprecipitated from cell lysates or detergent-dissolved virions and analyzed by SDS-polyacrylamide gel electrophoresis (SDS-PAGE) as previously reported (41). After electrophoresis, the gels were processed for fluorography as previously reported (43) and exposed at −80°C to Kodak X-ray films or, for quantitative analyses, to storage phosphorimaging plates (Molecular Dynamics).

RNA isolation and reverse transcription-PCR (RT-PCR). At 6 h after transfection with synthetic EAV RNAs, BHK-21 C13 cells were extensively washed with prewarmed phosphate-buffered saline (PBS) containing 50 mM $CaCl_2$ and 50 mM $MgCl_2$ (PBS Ca/Mg) and given prewarmed GMEM–10% FBS. At 14 h p.t., the viral particles in the culture supernatant were pelleted though a 20% (wt/wt) sucrose cushion in TM as described above. The pellet was dissolved in TNM buffer (20 mM Tris-HCl [pH 7.6], 50 mM NaCl, 5 mM $MgCl_2$). Next, a 70-μl aliquot of the sample was mixed with 1 μl of DNase I (2 U/μl; Ambion), 1 μl of RNase A (36 mg/ml; Roche), 0.7 μl of Triton X-100, and 3.5 μl of 10% SDS. A second 70-μl aliquot was supplemented with 1 μl of DNase I, 1 μl of RNase A, and 4.2 μl of TNM buffer. After incubation for 1 h at 37°C, the enzymes were inactivated by the addition of 63.8 μl of 0.04% proteinase K (Roche) in TNM buffer and incubation for 30 min at 50°C. Subsequently, RNA was isolated from each sample by using a QIAamp viral RNA kit (QIAGEN) according to the instructions of the manufacturer. Reverse transcription was performed under standard conditions by using Moloney murine leukemia virus reverse transcriptase (Gibco-BRL) and the EAV ORF 5-specific primer A3 (5′-CCGCTGTAAATGCCATAG-3′, nucleotides 11627 through 11610 of the EAV untranslated region [Utr]) (5, 15). Subsequently, the cDNA was amplified by PCR by using oligonucleotides 112 (5′-GATGTCTATGCTCCATCATT-3′, located in ORF1b of the EAV Utr at positions 9263 through 9282) and 114 (5′-GCTCTTGTGGGTATTGACTC-3′, located in ORF2b of the EAV Utr at positions 10192 through 10211). Finally, the PCR products were purified by using a QIAquick PCR purification kit (QIAGEN), subjected to restriction enzyme digestion, and analyzed by agarose gel electrophoresis.

Electron microscopy of viral particles. BHK-21 C13 cells were transfected with synthetic EAV RNAs as described above. After 5 h of incubation, the cells were washed twice with prewarmed GMEM–10% FBS and incubated further in the same medium. The cell culture fluids were collected at 15 h p.t. and spun for 25 min at 6,500 × *g* to pellet cell debris. The cleared supernatants were layered onto a 20% (wt/wt) sucrose cushion made up in TM. After centrifugation for 2 h in an SW 50.1 rotor (Beckman) at 28,000 rpm and 4°C, the pellets were suspended in 20 mM Tris-HCl (pH 7.4)–100 mM NaCl–1 mM EDTA–1% FBS and subsequently stored at 4°C. The virus suspension was mounted on a Formvar-coated copper grid and incubated with the mouse MAb 93B (1:5), followed by rabbit anti-mouse immunoglobulin G (1:200) (DakoCytomation, Denmark) and 10-nm protein A-colloidal gold particles. The grids were negatively stained with uranyl acetate.

Electron microscopy of cells transfected with synthetic EAV RNAs. BHK-21 C13 cells were transfected with synthetic EAV RNAs as described above. For conventional transmission electron microscopy (TEM), the cells were fixed 14 h after transfection by a 60-min incubation at RT with 1.5% glutaraldehyde in cacodylate buffer for 60 min at RT. The cells were washed twice in PBS and postfixed with 1% osmium tetroxide in cacodylate buffer for 90 min at 4°C. After two rinses with PBS, the cells were dehydrated with ethanol in a stepwise fashion. The cells were embedded in epoxy resin X-112 (Ladd Research Industries) and polymerized for 72 h at 60°C. Ultrathin sections were stained with uranyl acetate and a saturated solution of lead hydroxide.

For immunoelectron microscopy (IEM), the cells were fixed with 2% paraformaldehyde in PHEM buffer (60 mM piperazine-1,4-bis[2-ethanesulfonic acid], 25 mM HEPES, 2 mM $MgCl_2$, 10 mM EGTA adjusted to a pH of 6.9 with NaOH) for 24 h at RT. After washing in PBS, the cells were pelleted and embedded in 12% gelatin. The pellet was cut into 1-mm^3 cubes, cryoprotected in 2.3 M sucrose, and snap-frozen in liquid nitrogen. Ultrathin cryosections were labeled with one of the mouse MAbs 51A (1:3) or E1A19 (1:3) or with the rabbit polyclonal antiserum αN (1:1,000). The rabbit polyclonal serum was labeled with 10-nm protein A-gold particles. The mouse MAbs were indirectly labeled with 10-nm protein A-gold particles via a rabbit anti-mouse immunoglobulin G bridging antibody (1:200). The grids were contrasted with uranyl acetate and embedded in methylcellulose.

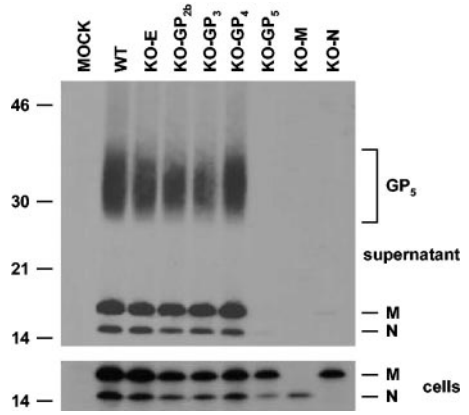

FIG. 1. Structural protein requirements in EAV assembly. BHK-21 cells were either mock-transfected or transfected with in vitro transcripts derived from the genomic EAV constructs indicated on top of the fluorograph. At 7 h p.t., the cells were labeled with [^{35}S]methionine. After incubation for 12 h at 39°C, the cells and supernatants were separately harvested. Cell lysates were prepared and subjected to immunoprecipitation with αM and αGP$_5$ (lower panel). After removal of cell debris by low-speed centrifugation, the viral particles present in the culture supernatant were pelleted through a cushion of 20% (wt/wt) sucrose. The pellet was then dissolved in lysis buffer and subjected to immunoprecipitation with αM and αGP$_5$ (upper panel). The samples were finally dissolved in Laemmli sample buffer and analyzed under reducing conditions by SDS–15% PAGE. The values on the left are the molecular sizes, in kilodaltons, of marker proteins analyzed in the same gel.

All electron microscopy specimens were viewed with a Philips EM 410 LS transmission electron microscope (Eindhoven, The Netherlands) at 80 kV.

RESULTS

EAV structural proteins required for particle assembly. To determine which of the EAV structural proteins are required for particle formation, we used seven different mutant infectious cDNA clones. In these clones, which were designated KO-E, KO-GP$_{2b}$, KO-GP$_3$, KO-GP$_4$, KO5-GP$_5$, KO-M, and KO-N, the ORFs encoding the indicated structural proteins were disrupted (21, 27, 32). In vitro transcripts derived from each of these genomic EAV constructs or from the WT infectious cDNA clone of EAV were transfected into BHK-21 cells by electroporation. At 7 h p.t., the cells were labeled for 12 h with [^{35}S]methionine. The cells and culture supernatants were then harvested separately. The particulate material in the culture supernatants was concentrated by sedimentation through a 20% (wt/wt) sucrose cushion and dissolved in lysis buffer while the cells were directly mixed with lysis buffer. Next, the intra- and extracellular material was incubated with antibodies specific for the major envelope proteins of EAV and analyzed by SDS-PAGE. No antiserum was used to precipitate the EAV N protein, as it binds directly to the formalin-fixed and heat-inactivated *Staphylococcus aureus* cells used to collect the specific immune complexes (31).

As is shown in the lower panel of Fig. 1, the N and M proteins were clearly observed in all cell lysates, with the exception of those derived from cells transfected with KO-M and KO-N RNA, respectively. Likewise, the GP$_5$ protein was detected in each cell lysate, except for that of KO-GP$_5$ RNA-transfected cells. However, because of the relatively high background signals in the parts of the gel containing the GP$_5$ protein and its heterogeneous N glycosylation, only the intracellular M and N proteins are displayed in Fig. 1.

The analysis of the culture supernatants (Fig. 1, upper panel) revealed that without N, M, or GP$_5$, no viral particles were secreted, as shown by the absence of each of them in the pellets derived from the culture supernatants of KO-GP$_5$, KO-M, and KO-N RNA-transfected cells. In contrast, inactivation of any of the other structural protein genes did not block secretion of the three major virion proteins. For KO-E, KO-GP$_{2b}$, KO-GP$_3$, and KO-GP$_4$, comparable amounts of the N, M, and GP$_5$ proteins were immunoprecipitated. Viral particles were also detected in the culture medium of BHK-21 cells transfected with synthetic RNAs transcribed from an EAV cDNA clone in which ORFs 2a, 2b, and 3 and the first 26 nucleotides of ORF 4 (i.e., nucleotides 9756 to 10723 of the EAV Utr) were deleted (data not shown). We hence conclude that the EAV E, GP$_{2b}$, GP$_3$, and GP$_4$ proteins are not essential for particle formation.

Protein composition of the viral particles produced in the absence of the minor envelope proteins. To obtain a complete picture of the structural protein composition of the viral particles released in the absence of E, GP$_{2b}$, GP$_3$, and GP$_4$, cells transfected with KO-E, KO-GP$_{2b}$, KO-GP$_3$, or KO-GP$_4$ RNA were again metabolically labeled. However, to improve the detection of the GP$_3$ and GP$_4$ proteins, this time the labeling procedure was performed with [^{35}S]cysteine instead of [^{35}S]methionine. After labeling, the culture supernatants were mixed with concentrated lysis buffer, and immunoprecipitations were performed with antisera specific for E, GP$_{2b}$, GP$_3$, and GP$_4$ in the presence of 5 mM dithiothreitol. The resulting

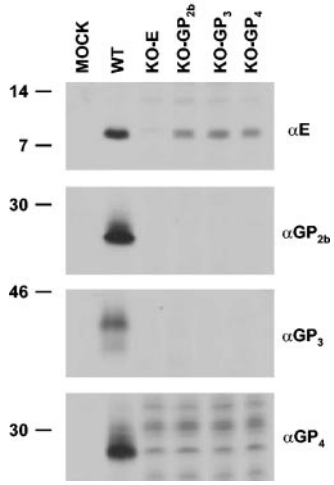

FIG. 2. Presence of the minor envelope proteins in viral particles. BHK-21 cells were transfected with in vitro transcripts derived from the EAV cDNA clones WT, KO-GP$_{2b}$, KO-GP$_3$, or KO-GP$_4$. At 7 h p.t., the cells were labeled with [^{35}S]cysteine for 12 h. After removal of cell debris by low-speed centrifugation, the viral particles present in the culture medium were dissolved in lysis buffer and subjected to immunoprecipitation with αE, αGP$_{2b}$, αGP$_3$, or αGP$_4$ in the presence of 5 mM dithiothreitol. The immunoprecipitates were analyzed under reducing conditions by SDS–20% PAGE (αE) or SDS–15% PAGE (αGP$_{2b}$, αGP$_3$, and αGP$_4$). The values on the left are the molecular sizes, in kilodaltons, of marker proteins analyzed in the same gel.

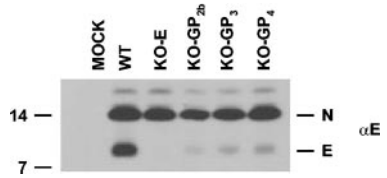

FIG. 3. Quantification of the E protein in viral particles. [^{35}S]methionine-labeled WT, KO-E, KO-GP_{2b}, KO-GP_3 and KO-GP_4 particles were generated and processed as described in the legend of Fig. 1 and incubated with αE. After immunoprecipitation the samples were dissolved in Laemmli sample buffer and analyzed under reducing conditions by SDS–20% PAGE.

immunoprecipitates were analyzed by SDS-PAGE under reducing conditions (Fig. 2).

While all the minor envelope proteins were clearly detectable in the control sample derived from WT RNA-transfected cells, the absence of the E protein abolished the appearance in the culture medium of GP_{2b}, GP_3, and GP_4. The lack of any of the minor envelope glycoproteins completely inhibited the secretion of the remaining two and greatly reduced the amount of E protein in the culture supernatant. Several protein species were immunoprecipitated by αGP_4 from the supernatant of WT RNA-transfected cells in addition to the GP_4 protein. Since these polypeptides were also observed in samples derived from KO-E, KO-GP_2, and KO-GP_3 RNA-transfected cells but not in the supernatant of mock-transfected cells, they most likely represent cellular proteins released as a consequence of EAV-related cytotoxicity. The three minor envelope glycoproteins thus require each other as well as the E protein to become incorporated into viral particles. Conversely, the absence of any of the three minor envelope glycoproteins hampers but does not completely block the incorporation of the E protein into viral particles.

The goal of the next experiment was to better compare the relative abundance of the EAV E protein in WT virions with that in the viral particles released from KO-E, KO-GP_{2b}, KO-GP_3, or KO-GP_4 RNA-transfected cells. For this purpose, [^{35}S]methionine-labeled extracellular material from the first experiment was subjected to immunoprecipitation with αE and analyzed by SDS-PAGE under reducing conditions. The resulting gel (Fig. 3) was analyzed with a phosphorimager to determine the E/N ratio of each sample. It turned out that the E protein was approximately fivefold less abundant in the viral particles obtained with KO-GP_{2b}, KO-GP_3, and KO-GP_4 than in WT virions.

GP_5/M heterodimerization in the absence of the minor envelope proteins. In WT EAV particles the GP_5 and M protein occur as disulfide-bonded heterodimers. To study whether the same holds true for the viral particles generated in the absence of the minor envelope proteins, [^{35}S]cysteine-labeled extracellular material from the second experiment was incubated with a mixture of M- and GP_5-specific antibodies. The resulting immunoprecipitates were analyzed by SDS–15% PAGE under nonreducing conditions. As is shown in Fig. 4, a protein species migrating at a molecular size position of 40 to 46 kDa, which fits with the previously reported electrophoretic mobility of the GP_5/M heterodimers (7), was brought down in each instance. Furthermore, in none of the samples were M or GP_5 monomers detected. Thus, both in WT virions and in viral particles

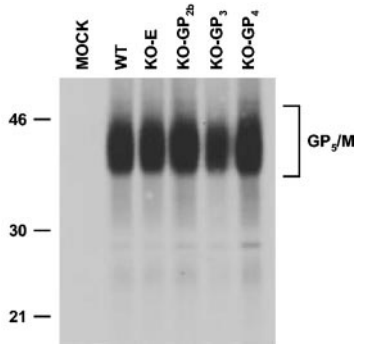

FIG. 4. GP_5/M heterodimer formation in viral particles. [^{35}S]cysteine-labeled WT, KO-E, KO-GP_{2b}, KO-GP_3, and KO-GP_4 particles were generated and processed as described in the legend of Fig. 2 and incubated with αM. After immunoprecipitation the samples were analyzed by SDS-PAGE under nonreducing conditions. The values on the left are the molecular sizes, in kilodaltons, of marker proteins analyzed in the same gel.

derived from KO-E, KO-GP_{2b}, KO-GP_3, or KO-GP_4 RNA-transfected cells, the EAV GP_5 and M proteins are exclusively present as covalently linked heterodimers.

RNA encapsidation in the absence of the minor envelope proteins. Since the viral particles lacking the E, GP_{2b}, GP_3, and GP_4 proteins are not infectious (21, 27), it was of interest to assess whether they contain viral genomic RNA. Thus, the viral particles secreted by KO-E RNA-transfected cells were subjected to RT-PCR. Virions released from WT RNA-transfected cells served as a positive control. Prior to reverse transcription, the viral particles were incubated with RNase A and DNase I, as described in Materials and Methods. These treatments were carried out to ensure that only RNA molecules incorporated into viral particles would serve as templates for RT-PCR. As a control for the activities of both nucleases, a digestion was also performed in the presence of Triton X-100 and SDS. Next, the enzymes were degraded with proteinase K, RNA was extracted from both samples, and RT-PCRs were carried out by using EAV-specific oligonucleotides. These oligonucleotides should yield a PCR product of 948 bp, which in

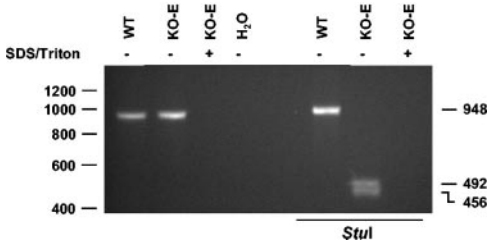

FIG. 5. Packaging of genomic EAV RNA in viral particles. KO-E particles were treated with DNase I and RNase A in the presence or absence of SDS and Triton X-100. After inactivation of these enzymes by proteinase K, RNA was isolated from each sample and used for RT-PCR with primers located at either side of the StuI site that was introduced as a marker mutation in the KO-E RNA. When indicated, the PCR fragments were digested with StuI. The reaction products were analyzed by agarose gel electrophoresis. The numbers on the right refer to the anticipated sizes of the PCR fragments before and after StuI digestion. On the left, the positions and sizes of marker DNA fragments that were analyzed in the same gel are indicated (in nucleotides).

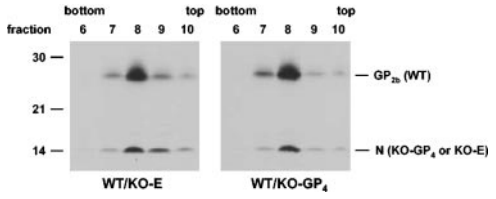

FIG. 6. Buoyant density of viral particles. BHK-21 cells were transfected with in vitro transcripts derived from WT, KO-E, or KO-GP_4. At 7 h p.t., the cells were labeled for 7 h with [^{35}S]methionine (WT) or [^{35}S]cysteine (KO-E and KO-GP_4). After the removal of cell debris by low-speed centrifugation, a 200-μl aliquot of the supernatant of WT RNA-transfected cells was mixed with a 200-μl aliquot of the supernatant of the KO-E or KO-GP_4 RNA-transfected cells. The mixtures were loaded onto 20 to 50% (wt/wt) sucrose density gradients. After centrifugation for 16 h at 30,000 rpm and 4°C in an SW 41 rotor, the gradients were fractionated and each fraction was incubated with αGP_{2b}. The resulting immunoprecipitates were analyzed by SDS–15% PAGE under reducing conditions. The numbers of the gradient fractions are indicated at the top. The values on the left are the molecular sizes, in kilodaltons, of marker proteins analyzed in the same gel.

the case of KO-E should contain an internal StuI site (27). As shown in Fig. 5, for both samples a PCR fragment of the expected length was observed when the treatment with RNase A and DNase I was performed in the absence of detergents, whereas no PCR product was obtained when Triton X-100 and SDS were added together with the nucleases. Incubation of the PCR fragments with StuI confirmed their authenticity; that is, while the PCR product derived from WT EAV particles was not affected by the restriction enzyme, the KO-E-specific PCR fragment was cleaved into the predicted fragments of 456 and 492 bp. These results demonstrate that viral genomic RNA was present inside the viral particles generated in the absence of the EAV E protein.

Buoyant density of the viral particles produced in the absence of the minor envelope proteins. In the next experiment, equilibrium sucrose density gradient centrifugation was used to compare the buoyant density of WT virions with that of viral particles lacking most or all of the minor envelope proteins. To this end, [^{35}S]cysteine-labeled WT EAV particles were mixed with [^{35}S]methionine-labeled KO-E or KO-GP_4 particles and loaded on a 20 to 50% sucrose gradient. After centrifugation, the gradients were fractionated and each fraction was incubated with αGP_{2b}. The resulting immunoprecipitates were analyzed by SDS-PAGE under reducing conditions (Fig. 6). The GP_{2b} protein is absent in the KO-E and KO-GP_4 particles and, thus, marks the position in the gradient of the WT virions, while the N protein indicates the position of the KO-E and KO-GP_4 particles, as it does not contain cysteine residues. As is shown in the left panel of Fig. 6, the KO-E and WT EAV particles occupied identical positions in the gradient at a buoyant density of approximately 1.15 g/ml. The same was true for WT virions and KO-GP_4 particles (Fig. 6, right panel). These observations imply that the viral particles generated in the absence of the EAV E or GP_4 proteins have the same buoyant density as WT virions.

Electron microscopic analysis of viral EAV particles. Finally, the electron microscopic appearance of KO-E particles was compared with that of WT virions. In vitro transcripts derived from KO-E and WT particles were transfected into BHK-21 cells. At 15 h p.t., the material released into the supernatant was concentrated through a 20% (wt/wt) sucrose cushion and studied by electron microscopy. EAV particles were identified by immunogold labeling with MAb 93B as the primary antibody. Labeled particles were observed in the material pelleted from the supernatants of the cells transfected with either WT (Fig. 7, upper panels) or KO-E (Fig. 7, lower panels) RNA. The KO-E particles had the same dimensions and appearance as the WT virions.

Electron microscopic analysis of KO-GP_5, KO-M, and KO-N RNA-transfected cells. To obtain more insight into the intracellular assembly process of EAV, BHK-21 cells were transfected with synthetic RNAs transcribed from WT, KO-GP_5, KO-M, and KO-N particles. At 14 h p.t., the cells were processed for TEM. The WT RNA-transfected cells displayed a number of characteristic alterations compared to mock-transfected control cells. In some areas of the cytoplasm, very high numbers of free ribosomes were detected. Sections through these regions often showed small fragments of the ER. The characteristic double-membrane vesicles (23, 28) were also present, as were smooth spherical forms and numerous tubular structures (Fig. 8A). These long electron-lucent cylindrical shapes had a diameter of approximately 50 nm. Similar tubules were previously observed by others in EAV-infected BHK-21 cells and in tissues from EAV-infected horses (2, 11, 36). Unfortunately, the detection of EAV particles was obscured by the occurrence of endogenous viral structures, which were also observed in the mock-transfected cells. The presence of such structures in BHK-21 cells has been reported previously (19, 22, 37). Moreover, in contrast to what was reported in other studies (20, 36), nucleocapsids were not observed in the cytoplasm at the time points investigated (12, 14, and 16 h p.t.).

Two notable differences were observed between WT RNA-transfected BHK-21 cells and BHK-21 cells transfected with the mutant EAV genomes. The tubular structures detected in the cells undergoing WT EAV infection were completely absent in the KO-N RNA-transfected cells (data not shown) and were more profuse in the KO-GP_5 and KO-M RNA-transfected cells (Fig. 8B and data not shown). Furthermore, occasionally rod-shaped forms were observed in the KO-M RNA-transfected cells (Fig. 8C and D) but not in the mock-transfected cells or in the cells that had received WT, KO-GP_5, or KO-N RNA. These structures were mainly found in ER-

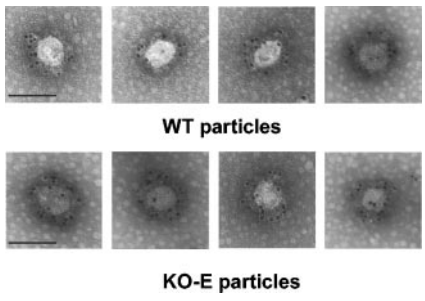

FIG. 7. Electron microscopy of KO-E particles. Particles secreted from WT (upper panels) and KO-E (lower panels) RNA-transfected cells were concentrated by pelleting through a 20% (wt/wt) sucrose cushion. Particles were viewed by electron microscopy after immunogold labeling with the GP_5-specific MAb 93B (14) and a protein A-gold conjugate. Bar, 100 nm.

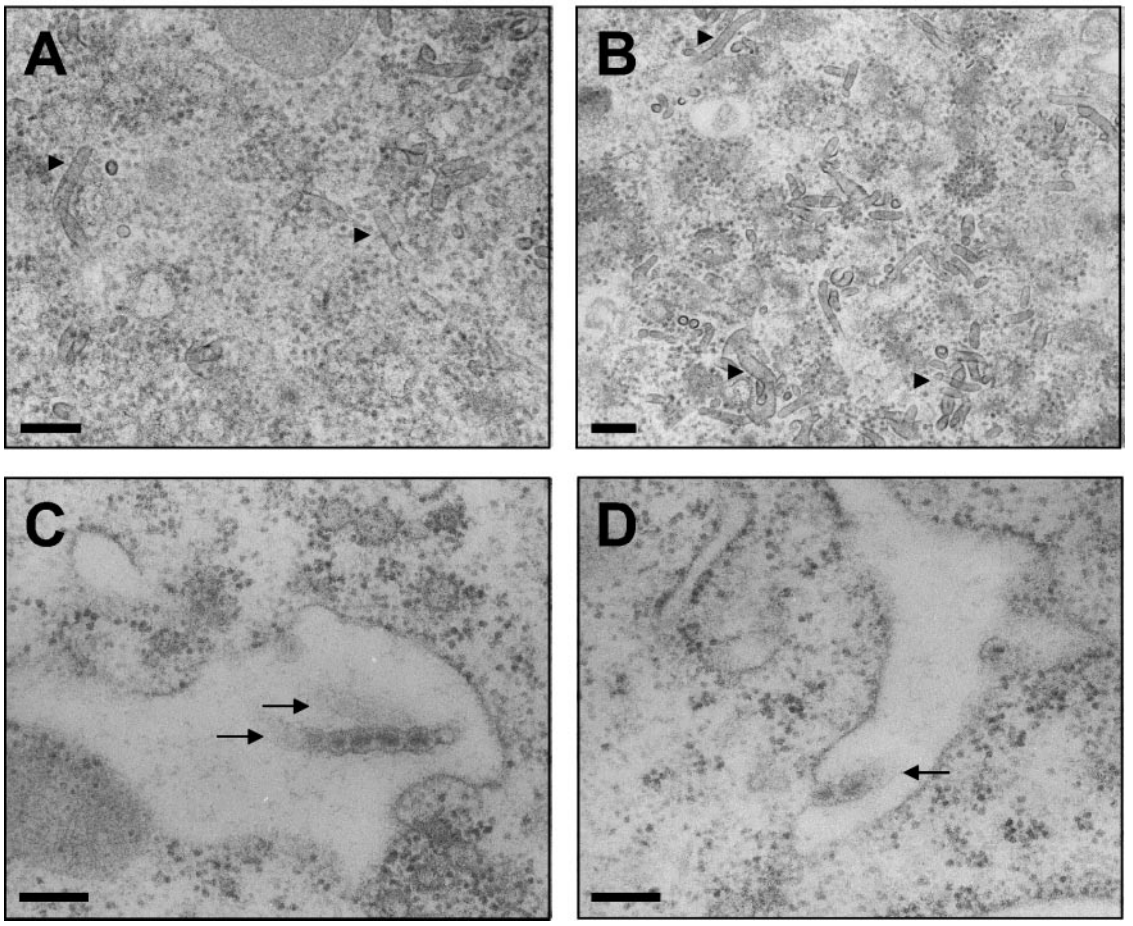

FIG. 8. Transmission electron micrographs of ultrathin sections of BHK-21 cells transfected with in vitro transcripts derived from the WT (A), KO-GP_5 (B), or KO-M (C and D) cDNA clones. The arrowheads in panels A and B point to some of the characteristic tubular structures; the arrows in panels C and D mark typical virus chains situated in the lumen of ER-associated vesicles. Bar, 200 nm.

associated vesicles located in the ribosome-rich areas. It seemed as if these membrane-surrounded rod-shaped forms contain multiple viral cores. For this reason, we refer to them as "virus chains." The diameters of these virus chains and their inner cores closely approximated those of mature extracellular particles and nucleocapsids of EAV, respectively.

Since the EAV-specific cytoplasmic tubules were not found in KO-N RNA-transfected cells, we were interested whether these structures actually contain the N protein. To this end, BHK-21 cells were transfected with synthetic RNAs transcribed from the WT and KO-N EAV cDNA clones. At 14 h p.t., the cells were processed for IEM by using different N-specific antibodies. Unfortunately, the EAV-specific tubular structures could not be unambiguously identified in the IEM preparations. It was, therefore, impossible to decide whether they are recognized by N-specific antibodies and, hence, contain the N protein. However, the IEM still yielded some interesting results. The N-specific MAbs E1A19 and 51A, produced through immunization of mice with purified EAV particles, were typically present in clusters in the cytoplasm of WT RNA-transfected cells (Fig. 9A and B). On the basis of their size and shape, we speculate that these clusters represent nucleocapsids. MAbs E1A19 and 51A, thus, most likely recognize epitopes not displayed by the N protein located in the cell nucleus and most of the cytoplasmic N molecules. In contrast, the polyclonal αN antiserum, generated by immunization of a rabbit with bacterially expressed full-length N protein, recognized antigens in the cytoplasm as well as in the nucleus of WT RNA-transfected cells (Fig. 9C) but did not label cells transfected with KO-N RNA (data not shown). The nuclear staining observed with αN is consistent with previous immunofluorescence studies, in which part of the EAV N protein was shown to reside in nucleoli (30).

DISCUSSION

In the present study, we used a reverse genetics approach to investigate which EAV structural proteins are required for particle assembly. Our experiments showed that the major envelope proteins, GP_5 and M, and the nucleocapsid protein N are essential for the formation of EAV particles. None of the other structural proteins, E, GP_{2b}, GP_3, and GP_4, is required to generate viral particles. The viral particles produced in the absence of the E protein or one of the minor envelope glycoproteins did contain viral genomic RNA and had the same

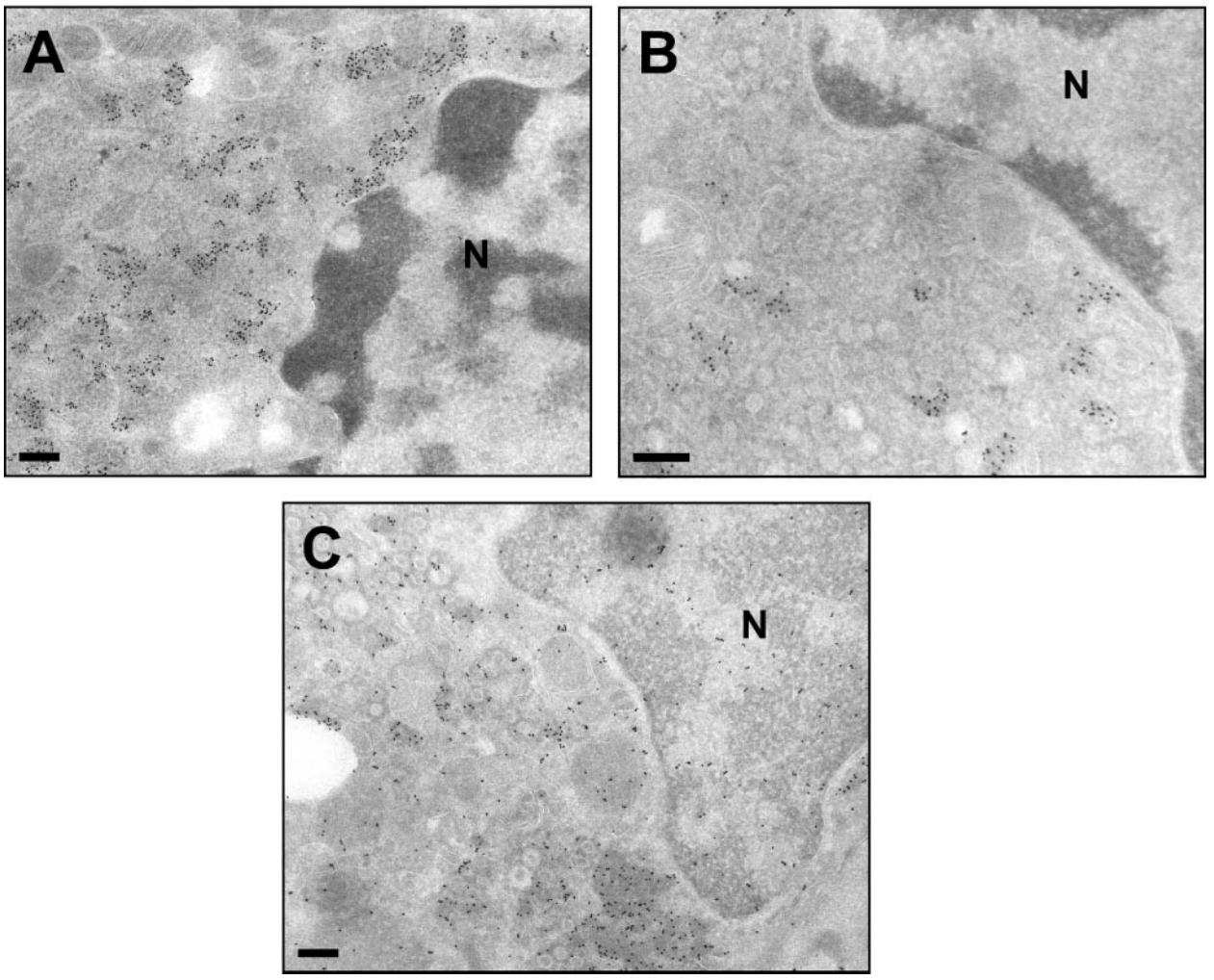

FIG. 9. Immunoelectron micrographs of ultrathin sections of BHK-21 cells transfected with in vitro transcripts derived from the WT cDNA clone. WT RNA-transfected cells were labeled with the N-specific MAbs E1A19 (A) and 51A (B) or the polyclonal antiserum αN (C). Both MAbs only recognize cytoplasmic structures and occur in clusters. In contrast, αN staining was observed in the cytoplasm as well as the nucleus. N, nucleus; bar, 200 nm.

buoyant density, electron microscopic appearance, and major structural protein composition as WT virions.

Nidoviruses have been grouped together on the basis of conserved amino acid sequence motifs in their polymerase (poly)proteins and similarities in their genome organization and gene expression strategy (4). However, members of the three nidovirus families (i.e., *Arteriviridae*, *Coronoviridae*, and *Roniviridae*) differ greatly in their virion architecture and in the nature of their structural proteins. The only structural feature shared by all vertebrate nidoviruses is the presence in virions of relatively large amounts of a triple-spanning membrane protein (25). For coronaviruses, this so-called M protein has been demonstrated to be essential for virus assembly (33), but little is known about its function in other nidoviruses. Our observation that no EAV particles are secreted in the absence of M demonstrates that this protein also plays a pivotal role in the assembly of arteriviruses.

In the present study, we have demonstrated that the assembly of secretion-competent EAV particles depends on the presence of both the nucleocapsid protein and the major viral envelope proteins. In contrast, for coronaviruses the coexpression of the M and E genes is sufficient to form virus-like particles (VLPs) (33). This indicates a critical difference in virion assembly between arteriviruses and coronaviruses. Consistently, all attempts to produce VLPs by the cotransfection of cells with expression plasmids encoding the EAV GP_5, M, and N proteins failed (reference 27 and data not shown). Thus, the presence of a triple-spanning membrane protein does not automatically imply a nucleocapsid-independent mode of assembly. The failure to generate VLPs by the simultaneous expression of EAV ORF5, ORF6, and ORF7 suggests that there are additional factors involved in EAV particle formation. EAV assembly may, for instance, be coupled to viral genome replication or rely on specific interactions between viral (genomic) RNA sequences and one or more of the major structural proteins. The budding requirements of arteriviruses place them in the same category as togaviruses. In this respect it is interesting that EAV was initially classified as a togavirus on the basis of

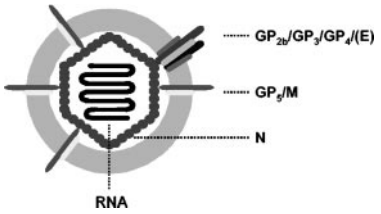

FIG. 10. Schematic model of an EAV particle. The genomic RNA is encapsidated by nucleocapsid protein molecules (N), forming a putatively icosahedral nucleocapsid. The envelope consists of a lipid bilayer in which the proteins GP_5 and M are predominant and occur as a disulfide-linked heterodimer. The minor envelope glycoproteins GP_{2b}, GP_3, and GP_4 form a heterotrimeric complex which interacts with a defined number of E molecules and is located above at the vertices of the isometric core.

the physicochemical properties, size, morphology, and protein composition, of its virions (24, 40).

An important finding of this study was the interdependence of the minor envelope glycoproteins and the E protein for their incorporation into viral particles. Moreover, it has recently been demonstrated that GP_{2b}, GP_3, and GP_4 form a complex in EAV-infected cells and appear in virions as disulfide-bonded heterotrimers (42). These observations strongly suggest that the minor envelope glycoproteins are jointly incorporated into virions. Our present results not only confirm this hypothesis but also indicate that the incorporation of the E protein is somehow linked to that of the $GP_{2b}/GP_3/GP_4$ heterotrimers. In the absence of the latter, the amount of E in viral particles is reduced by 60 to 80%. Conversely, in the absence of the E protein, none of the minor envelope glycoproteins is incorporated. EAV virions contain approximately 25 times less of the minor envelope glycoproteins than of the GP_5 and M proteins (6, 43), while intermediate amounts of the E protein are present in virus particles (27). These numbers, combined with the demonstrated occurrence of GP_5/M heterodimers (7) and $GP_{2b}/GP_3/GP_4$ heterotrimers (42) and considering the apparent interaction between E molecules, lead us to propose a new model of the EAV virion (Fig. 10). In this model the minor envelope glycoproteins are positioned in association with the E protein above the vertices of the putatively icosahedral nucleocapsid. Conceivably, the E protein is the component that through its interaction with the $GP_{2b}/GP_3/GP_4$ heterotrimer, on the one hand, and the GP_5/M heterodimers and/or the nucleocapsid, on the other hand, draws the complex of the minor envelope glycoproteins into nascent particles. The observation that the E, GP_{2b}, GP_3, and GP_4 proteins are not required for the formation of EAV particles, combined with the fact that these proteins are essential for conveying infectivity to these particles, lends further support to a role of the $GP_{2b}/GP_3/GP_4/(E)$ complex in the virus entry process.

The nucleocapsids synthesized in the cytoplasm of virus-infected cells are likely to bind to cytoplasmically exposed domains of envelope proteins in the process of viral budding. The finding that one can generate EAV particles devoid of the minor envelope glycoproteins and the E protein implies that the interaction between nucleocapsid and viral envelope is mediated by the disulfide-bonded GP_5/M heterodimers. It was recently shown that minor amino acid changes in the C terminus of GP_5 can block the formation of infectious PRRSV particles (35), suggesting that this domain is important for the interaction with the nucleocapsid or with other viral envelope proteins. Covalent association of the GP_5 and M proteins is essential for the production of infectious arteriviruses, as has been shown by mutation in EAV and PRRSV of the cysteines responsible for this association (26, 35). Moreover, the colocalization of the EAV GP_5 and M proteins in the Golgi apparatus correlates with the production of infectious virus and is dependent on this covalent interaction (9). It is, thus, quite likely that the formation of covalently linked GP_5/M heterodimers is a condition sine qua non for arterivirus particle formation. The transfection of BHK-21 cells with RNA encoding PRRSV mutants in which Cys-50 of GP_5 or the single cysteine of the M protein was replaced by a serine residue did not yield infectious viral progeny. Moreover, no PRRSV structural proteins or RNA molecules were detected in the supernatant of these cells in association with viral particles (34). On the other hand, arteriviruses appear surprisingly tolerant of deletions in and replacements of their GP_5 ectodomain. EAV deletion mutants lacking amino acids 66 through 112, 62 through 101, or 52 to 79 of GP_5 replicate in vitro (1, 3, 26). Moreover, replacement of the entire GP_5 ectodomain of EAV by that of PRRSV or LDV yielded replication-competent viruses (9). Likewise, Verheije et al. (35) demonstrated that the luminal domain of the PRRSV M protein could be replaced by that of EAV or LDV.

Our electron microscopic analyses revealed that the appearance in EAV-infected cells of the characteristic tubules seen by us and others (2, 11, 36) is dependent on the expression of the N protein; that is, no such structures were detected in the KO-N RNA-transfected cells. Unfortunately, we could not establish by IEM whether N is part of these tubules. Moreover, after independent expression of the N protein by a vaccinia virus vector (6), no tubules were observed (data not shown). Most likely, additional EAV components, e.g., replicating and/or encapsidation-competent-RNA and possibly also the viral replication complex, are required for the assembly of these structures. Alternatively, the intracellular milieu created by the recombinant vaccinia virus infection was not compatible with the formation of EAV-specific cytoplasmic tubules. However, Wada and coworkers (36) reported the labeling by N-specific MAbs of structures resembling the tubules observed in this study. The finding that the tubules were more abundant in cells transfected with KO-GP_5 or KO6-M RNA further supports a relationship with the N protein. The inability of nucleocapsids to bud in the absence of either the GP_5 or M protein supposedly leads to the accumulation of the N protein in the cytoplasm. Tubular structures are not uncommon in nidovirus-infected cells. They are also observed during infections of, for instance, LDV (29), mouse hepatitis virus (10), Breda virus (13, 18), and Berne virus (39). For all these viruses relationships were suggested between these tubules and viral cores.

The other remarkable structures observed by TEM were the virus chains seen in the ER of the KO-M RNA-transfected cells. We could not unequivocally determine whether these structures comprise EAV structural proteins. Nevertheless, it was clear that their formation in cells is related to the transfection with EAV RNA and is specifically dependent on the absence of the M protein as they were never detected in the

mock-transfected cells or cells transfected with WT, KO-GP_5, or KO-N RNA. Their appearance suggests that assembling virions were trapped at the ER membrane during the process of budding. These observations may point at a role for the M protein in the pinching off of budding virus particles and for the GP_5 endodomain in the interaction with the nucleocapsid. Similar viral chains were previously observed in electron micrographs of LDV-infected cells (29). In the case of LDV, the viral chains had the same maximum diameter as virus particles. Furthermore, the appearance of these structures was confined to later stages of infection, when massive amounts of viral proteins had been produced and the condition of the cells was quickly deteriorating.

ACKNOWLEDGMENTS

We thank Amy Glaser for donating MAbs 51A and 93B and Emilie and Frank Weiland for providing MAb E1A19.

REFERENCES

1. **Balasuriya, U. B. R., J. F. Patton, P. V. Rossitto, P. J. Timoney, W. H. McCollum, and N. J. MacLachlan.** 1997. Neutralization determinants of laboratory strains and field isolates of equine arteritis virus: identification of four neutralization sites in the amino-terminal ectodomain of the G_L envelope glycoprotein. Virology **232:**114–128.
2. **Breese, S. S. J., and W. H. McCollum.** 1971. Equine arteritis virus: ferritin-tagging and determination of ribonucleic acid core. Arch. Gesamte. Virusforsch. **35:**290–295.
3. **Castillo-Olivares, J., R. Wieringa, T. Bakonyi, A. A. F. de Vries, N. J. Davis-Poynter, and P. J. M. Rottier.** 2003. Generation of a candidate live marker vaccine for equine arteritis virus by deletion of the major virus neutralization domain. J. Virol. **77:**8470–8480.
4. **Cavanagh, D.** 1997. *Nidovirales*: a new order comprising *Coronaviridae* and *Arteriviridae.* Arch. Virol. **142:**629–633.
5. **den Boon, J. A., E. J. Snijder, E. D. Chirnside, A. A. F. de Vries, M. C. Horzinek, and W. J. M. Spaan.** 1991. Equine arteritis virus is not a togavirus but belongs to the coronaviruslike superfamily. J. Virol. **65:**2910–2920.
6. **de Vries, A. A. F., E. D. Chirnside, M. C. Horzinek, and P. J. M. Rottier.** 1992. Structural proteins of equine arteritis virus. J. Virol. **66:**6294–6303.
7. **de Vries, A. A. F., S. M. Post, M. J. B. Raamsman, M. C. Horzinek, and P. J. M. Rottier.** 1995. The two major envelope proteins of equine arteritis virus associate into disulfide-linked heterodimers. J. Virol. **69:**4668–4674.
8. **de Vries, A. A. F., M. J. B. Raamsman, H. A. van Dijk, M. C. Horzinek, and P. J. M. Rottier.** 1995. The small envelope glycoprotein (G_S) of equine arteritis virus folds into three distinct monomers and a disulfide-linked dimer. J. Virol. **69:**3441–3448.
9. **Dobbe, J. C., Y. van der Meer, W. J. M. Spaan, and E. J. Snijder.** 2001. Construction of chimeric arteriviruses reveals that the ectodomain of the major glycoprotein is not the main determinant of equine arteritis virus tropism in cell culture. Virology **288:**283–294.
10. **Dubois-Dalcq, M. E., E. W. Doller, M. V. Haspel, and K. V. Holmes.** 1982. Cell tropism and expression of mouse hepatitis viruses (MHV) in mouse spinal cord cultures. Virology **119:**317–331.
11. **Estes, P. C., and N. F. Cheville.** 1970. The ultrastructure of vascular lesions in equine viral arteritis. Am. J. Pathol. **58:**235–253.
12. **Faaberg, K. S., and P. G. W. Plagemann.** 1995. The envelope proteins of lactate dehydrogenase-elevating virus and their membrane topography. Virology **212:**512–525.
13. **Fagerland, J. A., J. F. Pohlenz, and G. N. Woode.** 1986. A morphological study of the replication of Breda virus (proposed family Toroviridae) in bovine intestinal cells. J. Gen. Virol. **67:**1293–1304.
14. **Glaser, A. L., A. A. F. de Vries, and E. J. Dubovi.** 1995. Comparison of equine arteritis virus isolates using neutralizing monoclonal antibodies and identification of sequence changes in G_L associated with neutralization resistance. J. Gen. Virol. **76:**2223–2233.
15. **Glaser, A. L., A. A. F. de Vries., M. J. B. Raamsman, M. C. Horzinek, and P. J. M. Rottier.** 1999. An infectious cDNA clone of equine arteritis virus: a tool for future fundamental studies and vaccine development, p. 166–176. *In* U. Wernery, J. F. Wade, J. A. Mumford, and O.-R. Kaaden (ed.), Proceedings of the 8th International Conference on Equine Infectious Diseases, Dubai 1998. R & W Publications, Ltd., New Market, England.
16. **Hedges, J. F., U. B. R. Balasuriya, and N. J. MacLachlan.** 1999. The open reading frame 3 of equine arteritis virus encodes an immunogenic glycosylated, integral membrane protein. Virology **264:**92–98.
17. **Horzinek, M. C., J. Maess, and R. Laufs.** 1971. Studies on the substructure of togaviruses. II. Analysis of equine arteritis, rubella, bovine viral diarrhea, and hog cholera viruses. Arch. Gesamte. Virusforsch. **33:**306–318.
18. **Horzinek, M. C., M. Weiss, and J. Ederveen.** 1987. Toroviridae: a proposed new family of enveloped RNA viruses. Ciba. Found. Symp. **128:**162–174.
19. **Lasneret, J., J. Lesser, L. Dianoux, M. Canivet, P. Bittoun, and J. Peries.** 1989. Electron microscopic characterisation of retrovirus and retrovirus-like particles induced by demethylating agents (5-azacytidine and 5-azadeoxycytidine) in Syrian hamster (Mesocricetus auratus) cells. J. Exp. Pathol. **4:**47–56.
20. **Magnusson, P., B. Hyllseth, and H. Marusyk.** 1970. Morphological studies on equine arteritis virus. Arch. Gesamte. Virusforsch. **30:**105–112.
21. **Molenkamp, R., H. van Tol, B. C. D. Rozier, Y. van der Meer, W. J. M. Spaan, and E. J. Snijder.** 2000. The arterivirus replicase is the only viral protein required for genome replication and subgenomic mRNA transcription. J. Gen. Virol. **81:**2491–2496.
22. **Payment, P., A. Chagnon, J. R. Cote, D. Ajdukovic, and V. Pavilanis.** 1972. Morphology of a latent virus associated with hamster cells BHK-21. Can. J. Microbiol. **18:**369–371.
23. **Pedersen, K. W., Y. van der Meer, N. Roos, and E. J. Snijder.** 1999. Open reading frame 1a-encoded subunits of the arterivirus replicase induce endoplasmic reticulum-derived double-membrane vesicles which carry the viral replication complex. J. Virol. **73:**2016–2026.
24. **Porterfield, J. S., J. Casals, M. P. Chumakov, S. Y. Gaidamovich, C. Hannoun, I. H. Holmes, M. C. Horzinek, M. Mussgay, N. Oker-Blom, P. K. Russell, and D. W. Trent.** 1978. Togaviridae. Intervirology **9:**129–148.
25. **Rottier, P.J.M.** 1995. The coronavirus membrane protein, p 115–139. *In* S. G. Siddell (ed.), The Coronaviridae. Plenum Press, New York.
26. **Snijder, E. J., J. C. Dobbe, and W. J. M. Spaan.** 2003. Heterodimerization of the two major envelope proteins is essential for arterivirus infectivity. J. Virol. **77:**97–104.
27. **Snijder, E. J., H. van Tol, K. W. Pedersen, M. J. B. Raamsman, and A. A. F. de Vries.** 1999. Identification of a novel structural protein of arteriviruses. J. Virol. **73:**6335–6345.
28. **Snijder, E. J., H. van Tol, N. Roos, and K. W. Pedersen.** 2001. Non-structural proteins 2 and 3 interact to modify host cell membranes during the formation of the arterivirus replication complex. J. Gen. Virol. **82:**985–994.
29. **Stueckemann, J. A., M. Holth, W. J. Swart, K. Kowalchyk, M. S. Smith, A. J. Wolstenholme, W. A. Cafruny, and P. G. W. Plagemann.** 1982. Replication of lactate dehydrogenase-elevating virus in macrophages. 2. Mechanism of persistent infection in mice and cell culture. J. Gen. Virol. **59:**263–272.
30. **Tijms M. A., Y. van der Meer, E. J. Snijder.** 2002. Nuclear localization of non-structural protein 1 and nucleocapsid protein of equine arteritis virus. J. Gen. Virol. **83:**795–800.
31. **van Berlo, M. F., J. J. W. Zeegers, M. C. Horzinek, and B. A. M. van der Zeijst.** 1983. Antigenic comparison of equine arteritis virus (EAV) and lactic dehydrogenase virus (LDV); binding of staphylococcal protein A to the nucleocapsid protein of EAV. Zentbl. Vetmed. Reihe B **30:**297–304.
32. **van Dinten, L. C., J. A. den Boon, A. L. M. Wassenaar, W. J. M. Spaan, and E. J. Snijder.** 1997. An infectious arterivirus cDNA clone: identification of a replicase point mutation that abolishes discontinuous mRNA transcription. Proc. Natl. Acad. Sci. USA **94:**991–996.
33. **Vennema, H., G. J. Godeke, J. W. A. Rossen, W. F. Voorhout, M. C. Horzinek, D. J. E. Opstelten, and P. J. M. Rottier.** 1996. Nucleocapsid-independent assembly of coronavirus-like particles by co-expression of viral envelope protein genes. EMBO J. **15:**2020–2028.
34. **Verheije, M. H.** 2002. Genetic engineering of the porcine reproductive and respiratory syndrome virus. Ph.D. thesis. Utrecht University, The Netherlands.
35. **Verheije, M. H., T. J. M. Welting, H. T. Jansen, P. J. M. Rottier, and J. J. M. Meulenberg.** 2002. Chimeric arteriviruses generated by swapping of the M protein ectodomain rule out a role of this domain in viral targeting. Virology **303:**364–373.
36. **Wada, R., Y. Fukunaga, T. Kondo, and T. Kanemaru.** 1995. Ultrastructure and immuno-cytochemistry of BHK-21 cells infected with a modified Bucyrus strain of equine arteritis virus. Arch. Virol. **140:**1173–1180.
37. **Wang, G., M. J. Mulligan, D. N. Baldwin, and M. L. Linial.** 1999. Endogenous virus of BHK-21 cells complicates electron microscopy studies of foamy virus maturation. J. Virol. **73:**8917.
38. **Weiland E, S. Bolz, F. Weiland, W. Herbst, M. J. B. Raamsman, P. J. M. Rottier, A. A. F. de Vries.** 2000. Monoclonal antibodies directed against conserved epitopes on the nucleocapsid protein and the major envelope glycoprotein of equine arteritis virus. J. Clin. Microbiol. **38:**2065–2075.
39. **Weiss, M., and M. C. Horzinek.** 1986. Morphogenesis of Berne virus (proposed family Toroviridae). J. Gen. Virol. **67:**1305–1314.
40. **Westaway, E. G., M. A. Brinton, S. Y. Gaidamovich, M. C. Horzinek, A. Igarashi, L. Kaariainen, D. K. Lvov, J. S. Porterfield, P. K. Russell, and D. W. Trent.** 1985. Togaviridae. Intervirology **24:**125–139.
41. **Wieringa, R., A. A. F. de Vries, S. M. Post, and P. J. M. Rottier.** 2003. Intra- and intermolecular disulfide bonds of the GP_{2b} glycoprotein of equine arteritis virus: relevance for virus assembly and infectivity. J. Virol. **77:**12996–13004.
42. **Wieringa, R., A. A. F. de Vries, and P. J. M. Rottier.** 2003. Formation of disulfide-linked complexes between the three minor envelope glycoproteins (GP_{2b}, GP_3, and GP_4) of equine arteritis virus. J. Virol. **77:**6216–6226.
43. **Wieringa, R., A. A. F. de Vries, M. J. B. Raamsman, and P. J. M. Rottier.** 2002. Characterization of two new structural glycoproteins, GP_3 and GP_4, of equine arteritis virus. J. Virol. **76:**10829–10840.